Dielectronic recombination of highly ionized iron

D. C. Griffin*
Joint Institute for Laboratory Astrophysics, University of Colorado and National Bureau of Standards, Boulder, Colorado 80309

M. S. Pindzola
Department of Physics, Auburn University, Auburn, Alabama 36849

(Received 20 October 1986)

Dielectronic recombination of the iron ions Fe^{15+}, Fe^{23+}, and Fe^{25+} has been studied in the isolated-resonance, distorted-wave approximation. The cross-section calculations include the dielectronic transitions associated with the $3s \rightarrow 3l$ and $3s \rightarrow 4l$ excitations in Fe^{15+}, the $2s \rightarrow 2p$ and $2s \rightarrow 3l$ excitations in Fe^{23+}, and the $1s \rightarrow 2l$ excitations in Fe^{25+}. The effects of external electric fields have been included by employing intermediate-coupled, field-mixed eigenvectors for the doubly excited Rydberg states, determined by diagonalizing a Hamiltonian matrix which includes the internal electrostatic and spin-orbit terms, as well as the Stark matrix elements. The field effects are found to be quite large in Fe^{15+}, relatively small in Fe^{23+}, and negligible in Fe^{25+}. The calculations indicate that there are large resonances near threshold in Fe^{23+} that are unaffected by external fields and may be measurable in new experiments currently being designed. In addition, the contributions of radiative recombination and the possible interference between radiative and dielectronic recombination in low-lying resonances are considered. Even though the radiative recombination cross sections may be appreciable near threshold in Fe^{15+} and Fe^{23+}, the interference between these processes appears to be completely negligible.

I. INTRODUCTION

Dielectronic recombination (DR) is expected to be the dominant recombination mechanism of positive ions with free electrons, and it can be described as a two-step process. In the first step, the electron collisionally excites the N-electron ion and is simultaneously captured into a doubly excited autoionizing state j of the $(N+1)$-electron ion:

$$e^- + X_i(Z,N) \rightarrow X_j^{**}(Z,N+1) . \quad (1)$$

If it emits a photon and decays to a bound state f,

$$X_j^{**}(Z,N+1) \rightarrow X_f(Z,N+1) + h\nu , \quad (2)$$

then the DR process is complete. However, the doubly excited state can also relax by autoionization to either the initial state i or some excited state k of the N-electron ion:

$$X_j^{**}(Z,N+1) \rightarrow X_k^{*}(Z,N) + e^- . \quad (3)$$

External field surely exist in all plasmas and electron-ion beam experiments. It has been demonstrated both experimentally[1] and theoretically[2-9] that such fields can significantly increase the magnitude of DR cross sections associated with $\Delta n = 0$ transitions, especially for ions in relatively low stages of ionization. In such cases the contributions from high principal quantum numbers are dominant, and the fields enhance the DR rates by redistributing the angular momentum among the Rydberg states in such a way as to open up many more recombination channels. However, such field effects should be far less pronounced for cases in which there are sizable contributions from low-lying resonances, where the energy separation between states with different values of angular momentum is much larger. Such dominance by low Rydberg states tends to occur in all $\Delta n \geq 1$ excitations, and for high stages of ionization, even in $\Delta n = 0$ excitations.

Previously, dielectronic-recombination-rate coefficients have been calculated for both sodiumlike iron[10] and lithiumlike iron[11,12] in the absence of an external field in pure LS coupling, and for lithiumlike iron in the presence of a field using the configuration-average approximation.[2] In addition, dielectronic satellite spectra have been calculated for hydrogenlike iron in intermediate coupling[13] The primary purpose of this work is to calculate intermediate-coupled DR cross sections and investigate the magnitude of electric-field enhancement of dielectronic recombination for Fe^{15+}, and Fe^{23+}, and Fe^{25+}. These results should provide some valuable insight into the significance of field effects in highly ionized systems, and, in addition, should be useful for future DR experiments currently being planned on these particular iron ions,[14] as well as similar highly ionized species.[15]

The remainder of this paper is arranged as follows. In Sec. II we give a brief outline of the theoretical methods. In Sec. III the results of our calculations of the DR cross sections are presented and discussed. Finally in Sec. IV we consider the implications of these results and the possible influence of two effects not included in the present calculations: interfering resonances in the presence of a field and the interference between radiative and dielectronic recombination.

II. THEORETICAL METHODS

A more complete description of the theoretical methods used in the present calculations is presented in Ref. 7.

Here we consider only the essentials of the theoretical and calculational methods employed. In the isolated-resonance approximation, the energy-averaged DR cross section from a state within the initial configuration of the N-electron ion to a particular state within the doubly excited configuration of the $(N+1)$-electron ion to all possible bound states of that ion is given by the expression

$$\bar{\sigma}=\frac{2\pi^2}{\Delta\varepsilon k_\varepsilon^2}\frac{1}{2G_I}\frac{\sum_i A_a(j\rightarrow i)\sum_f A_r(j\rightarrow f)}{\sum_k A_a(j\rightarrow k)+\sum_{f'} A_r(j\rightarrow f')} . \quad (4)$$

The above equation is in atomic units and $\Delta\varepsilon$ is an energy bin width larger than the largest resonance width, k_ε is the linear momentum of the continuum electron, and G_I is the total statistical weight of the initial configuration. The radiative rate $A_r(j\rightarrow f)$ from a particular doubly excited state to all states of a lower level $\gamma_f J_f$ in the $(N+1)$-electron ion is given by the equation

$$A_r(j\rightarrow f)=\frac{4\omega_{jf}^3}{3c^3}\sum_{M_f}\left|\left\langle \gamma_f J_f M_f \left| \sum_{m=1}^{N+1} \mathbf{r}_m \right| n_j l_j n\gamma_j M_j \right\rangle\right|^2 , \quad (5)$$

where ω_{jf} is the transition frequency, c is the speed of light, γ_f is used to designate all quantum numbers other than J_f and M_f which are needed to specify the final state in intermediate coupling, and we employ the dipole-length form of the electromagnetic interaction. In Eq. (4) f is used to designate bound levels only, while f' is used to signify any lower level, including autoionizing levels. In our calculations we include radiative transitions to lower autoionizing levels when the inner electron $n_j l_j$ is the active electron but ignore cascading transitions to lower autoionizing levels in which the Rydberg electron is the active electron. The validity of this approximation is discussed in Ref. 7.

The eigenvectors for the doubly excited states $|n_j l_j n\gamma_j M_j\rangle$ require some special comments. They represent autoionizing states in an electric field, consisting of a Rydberg electron outside of a single-core electron $n_j l_j$ (plus any number of electrons in closed subshells). They are determined by diagonalizing a Hamiltonian which includes the spin-orbit interactions, the electrostatic interactions of the Rydberg electron with the core, and the Stark matrix elements between states of opposite parity, but ignores internal electrostatic interactions between configurations and with the adjacent continua. The only rigorously conserved quantum number is M_j, the projection of the total angular momentum along the field direction. However, we also treat the principal quantum number n of the Rydberg electron as conserved; the validity of this approximation will be discussed in Sec. IV. Thus we express $|n_j l_j n\gamma_j M_j\rangle$ in terms of a basis set consisting of all possible states of the configurations $n_j l_j nl$ with $l=0,1,2,3,\ldots,n-1$, coupled according to the jK scheme, as follows:

$$|n_j l_j n\gamma_j M_j\rangle=\sum_{j_j,lK_j,J_j} Y_{j_j lK_j J_j}^{n_j l_j n\gamma_j M_j} |n_j l_j j_j nlK_j J_j M_j\rangle , \quad (6)$$

where γ_j is simply a serial number used to specify completely a given eigenvector, and j_j is the total angular momentum of the core. The jK coupling scheme is a convenient one since the Stark matrix element do not mix states with different values of j_j; thus j_j becomes a good quantum number as n increases and the electron-electron interactions of the Rydberg electron with the core and the spin-orbit interaction of the Rydberg electron decrease. For high values of n, the expansion in Eq. (6) includes hundreds of states, and a partition of them by j_j represents significant computational savings.

The autoionizing rate $A_a(j\rightarrow k)$ from a particular doubly excited state of the $(N+1)$-electron ion to all continuum states associated with a particular level of the N-electron ion is given by the expression

$$A_a(j\rightarrow k)=\frac{4}{k_\varepsilon}\sum_{l_\varepsilon,K_k,J_k,M_k}\left|\left\langle n_k l_k j_k k_\varepsilon l_\varepsilon K_k J_k M_k \left| \sum_{m=1}^{N}\frac{1}{r_{N+1,m}} \right| n_j l_j n\gamma_j M_j \right\rangle\right|^2 , \quad (7)$$

where l_ε is the angular momentum of the continuum electron, the bound states of the N-electron ion plus the continuum electron are designated in jK coupling, and the continuum normalization is one multiplied by a sine function. Complete expressions for the rates $A_r(j\rightarrow f)$ and $A_a(j\rightarrow k)$ are given in Ref. 7.

The majority of DR calculations presented in this paper were performed using a program DRFEUD[7] which calculates the dielectronic-recombination cross sections in the presence of an electric field using the above equations. However, for $\Delta n=1$ transitions to doubly excited configurations of the type $n_j l_j nl$ with $n=n_j$, where configuration interaction may be large and field effects are negligible, the multiconfiguration atomic structure program of Cowan[16] was employed to calculate DR cross sections to individual levels.

Finally, for the $\Delta n=1$ transitions of the type $3s\rightarrow 4lnl'$ in Fe^{15+}, it would have been quite difficult and enormously expensive to calculate these cross sections using the diagonalization technique inherent in the program DRFEUD. Since the cross sections for these transitions are dominated by the low-lying resonances, we instead employed the following technique. First, the cross sections for transitions to the configurations $4l4l'$ were calculated using the structure code, as described above. Then, for transitions to the multitude of configurations of the type $4lnl'$ with $n\geq 5$, the cross sections were calculated using the configuration-average, distorted-wave approximation program DRACULA.[4] In the absence of an external field, this method has been found to give results in good agreement with intermediate-coupled results,[17] such as those produced by DRFEUD. Maximum field effects are estimated

in DRACULA by transforming all autoionizing rates and those radiative rates for which the Rydberg electron is the active electron from a spherical to a parabolic basis.[4] However, since the cross section for these $\Delta n = 1$ transitions are dominated by the low-lying resonances, the field effects are negligible and this approximate method of estimating field effects has no effect on our final results.

In the present work we are not interested in determining the DR cross section as a function of electric-field strength in the interaction region as we were in earlier work;[7,8] here we are, instead, concerned only with the maximum effect of the field on the cross section. Therefore we have set the electric field at a very large value of 10 kV/cm. No additional change in the cross section would be expected in any of these ions with a further increase in the field strength. In most calculations, the energy bin width was set equal to 0.136 eV. This is larger than the largest resonance width and yet smaller than any expected experimental electron energy width.

In addition to mixing l states, the electric fields will ionize electrons in high Rydberg states. In an earlier study,[8] we included the effects of field ionization by employing the hydrogenic formula of Damburg and Kolosov.[18] The simplest method of including the effects of field ionization is to employ the semiclassical formula

$$n_{\max} = (6.2 \times 10^8 Q^3/F)^{1/4} \tag{8}$$

to determine the maximum principal quantum number above which field ionization will occur, where Q is the charge of the initial N-electron ion, and F is the electric-field strength in volts per centimeter. By comparison with results from the hydrogenic field-ionization formula, it is apparent that this equation provides a good estimate for high fields. Although they are expected to be large,[14] it is hard to estimate what the fields might be in the analyzing region in future DR experiments; therefore, we have arbitrarily set $n_{\max}$ to 100 in our calculations. This would correspond to an analyzing field of 21 kV/cm in Fe^{15+}, and 75 kV/cm in Fe^{23+}. (For Fe^{25+} the cross section is dominated by low-lying resonances and the cross section falls of rapidly with n; therefore, the value of $n_{\max}$ is not important.) The actual fields in the analyzing region should be larger than those in the interaction region, but may be smaller than the above values; however, it would be difficult for us to carry out a full diagonalization of the doubly excited Rydberg states much beyond $n = 100$.

III. CALCULATIONS FOR THE Fe IONS

A. Dielectronic recombination for Fe^{15+}

We first consider the $\Delta n = 0$ dielectronic-recombination transitions of the type $3s \rightarrow 3lnl'$ in sodiumlike iron. A schematic diagram of the energy levels for this system are shown in Fig. 1. Here we must consider three Rydberg series: $3p_{1/2}nl$, $3p_{3/2}nl$, and $3dnl$. The $3p_{1/2}nl$ sequence may autoionize to the initial $3s_{1/2}$ level for $n \geq 10$, and may radiate to the bound configurations $3snl$ and $3p_{1/2}n'l'$ for $n' \leq 9$. The $3p_{3/2}nl$ sequence may autoionize to the initial $3s_{1/2}$ level for $n \geq 10$ and also the $3p_{1/2}$ level for $n \geq 34$, and may radiate to the bound configurations $3snl$ and $3p_{3/2}n'l'$ for $n' \leq 9$. The $3p_{3/2}nl \rightarrow 3p_{1/2}$ intercombination autoionizing transitions are included in a natural way in our analysis since we employ a jK basis set for our intermediate-coupled, doubly excited Rydberg states. The radiative rates for the $3p \rightarrow 3s$ transitions (which we refer to as type 1) are nearly independent of n, and are not affected by an electric field. The radiative rates for the $nl \rightarrow n'l'$ transitions (which we refer to as type 2) fall off approximately as $1/n^3$ and are affected by external fields. These type-2 transitions (which have often been ignored in considerations of dielectronic recombination) have large rates for low Rydberg states in highly ionized systems, and it is these rates that are responsible for the size of the cross section at relatively low energies. The energy-averaged cross sections for the $3p_{1/2}nl$ and $3p_{3/2}nl$ sequences as a function of n are shown, with and without a field, in Fig. 2. As can be seen, the field effects are sizable and, when the intercombination autoionizing transition turns on at $n = 34$, there is a pronounced drop in the $3p_{3/2}nl$ cross section.

The $3dnl$ sequence for $n \geq 7$ can autoionize to the $3s_{1/2}$ level and for resonances of $3d\,8g$ and above can also autoionize to the $3p_{1/2}$ and $3p_{3/2}$ levels. The intercombina-

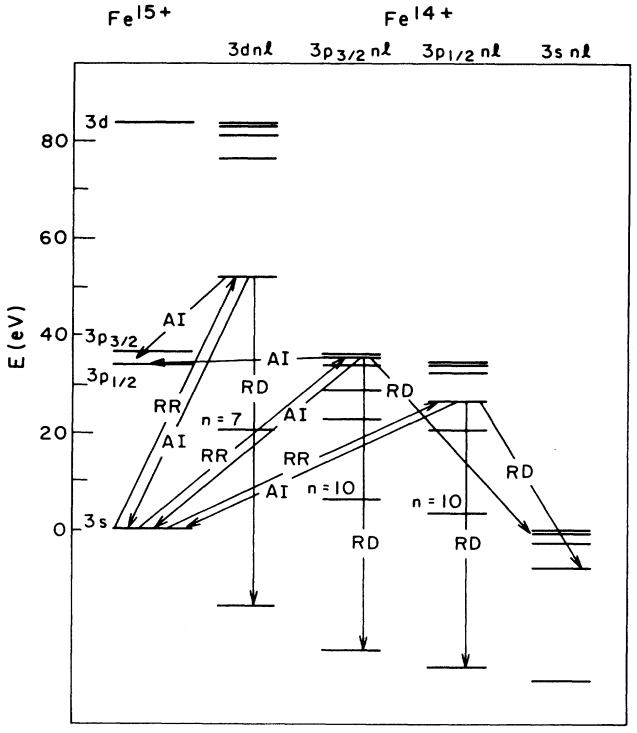

FIG. 1. Schematic energy-level diagram showing the transitions associated with $\Delta n = 0$ dielectronic recombination in Fe^{15+}. Here RR stands for resonant recombination into a doubley excited autoionizing state (not radiative recombination), AI stands for autoionization, and RD stands for radiative decay. Autoionization from the $3p_{3/2}nl$ configurations to the states of the $3p_{1/2}$ level begins at $n = 34$.

tion transitions $3d_{5/2}nl \rightarrow 3d_{3/2}$ can be ignored since the $3d$ spin-orbit splitting is so small that they would not begin to occur until $n = 92$, which is well beyond the point where these cross sections are appreciable. The $3dnl$ sequence can radiate to the bound configurations $3pnl$ for $7 \leq n \leq 9$ and $3dn'l'$ for $n' \leq 6$. As mentioned in Sec. II, the transitions $3dnl$ to the autoionizing configurations $3pnl$ for $n \geq 10$ are included in the total radiative rate which appears in the denominator of Eq. (4). The $3dnl$ configurations make a significant contribution to the cross section only for n equal to 7 and 8. Above this point, $3dnl \rightarrow 3p$ autoionizing transitions diminish the cross section significantly.

The energy-averaged cross section as a function of electron energy for the $\Delta n = 0$ transitions in Fe^{15+}, with and without an external electric field, is shown in the top portion of Fig. 3. The contributions from the $3p_{1/2}nl$ and $3p_{3/2}nl$ resonances approaching the series limits at 34.5 and 37.1 eV, respectively, are clearly visible. The contributions from the $3d\,7l$ resonances occur between 14.3 and 21.7 eV (with the largest peaks from 21.2 to 21.7 eV) and those from $3d\,8l$ appear between 31.5 and 36.0 eV. In the absence of a field, the low-lying resonances contribute significantly to the total cross section; however, when a strong field is turned on, the cross section is dominated by the high Rydberg states of the $3p_{1/2}nl$ and $3p_{3/2}nl$ sequences.

In the lower portion of Fig. 3, we show the energy-averaged cross sections convoluted with a 3-eV Gaussian to simulate a possible experimental electron-energy distribution. The separate $3p_{1/2}nl$ and $3p_{3/2}nl$ resonances are no longer visible, and the field enhancement in the high Rydberg states is seen to be about a factor of 5. However, the peak below 8 eV, due to the $3pnl$ resonances, and the peak just above 20 eV, due to the $3d\,7l$ configurations, should be visible in an experiment with such an electron distribution.

We now consider the contributions due to the $\Delta n = 1$ transitions in Fe^{15+}. A schematic energy-level diagram for this system is shown in Fig. 4. By far, the largest contributions to the cross section come from the $4l4l'$ com-

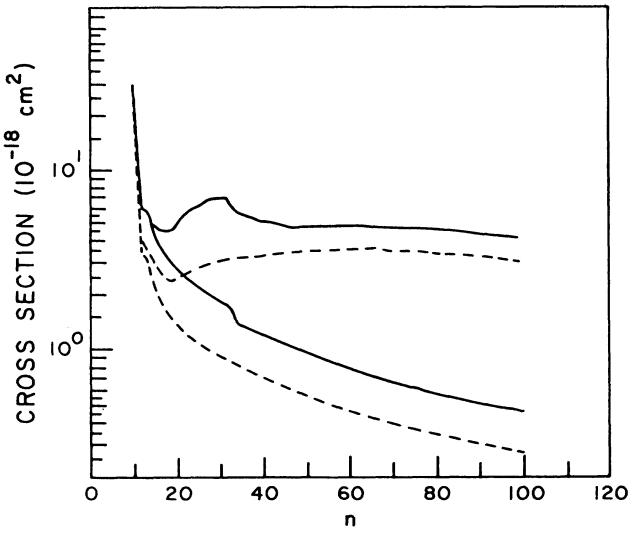

FIG. 2. Energy-averaged dielectronic-recombination cross sections associated with the $3s \rightarrow 3p_{1/2}$ and $3s \rightarrow 3p_{3/2}$ excitations in Fe^{15+} as a function of n. ——, curve for the $3p_{3/2}nl$ configurations; — — —, curve for the $3p_{1/2}nl$ configurations. The upper two curves are for a field of 10 kV/cm while the lower two curves are for no external field.

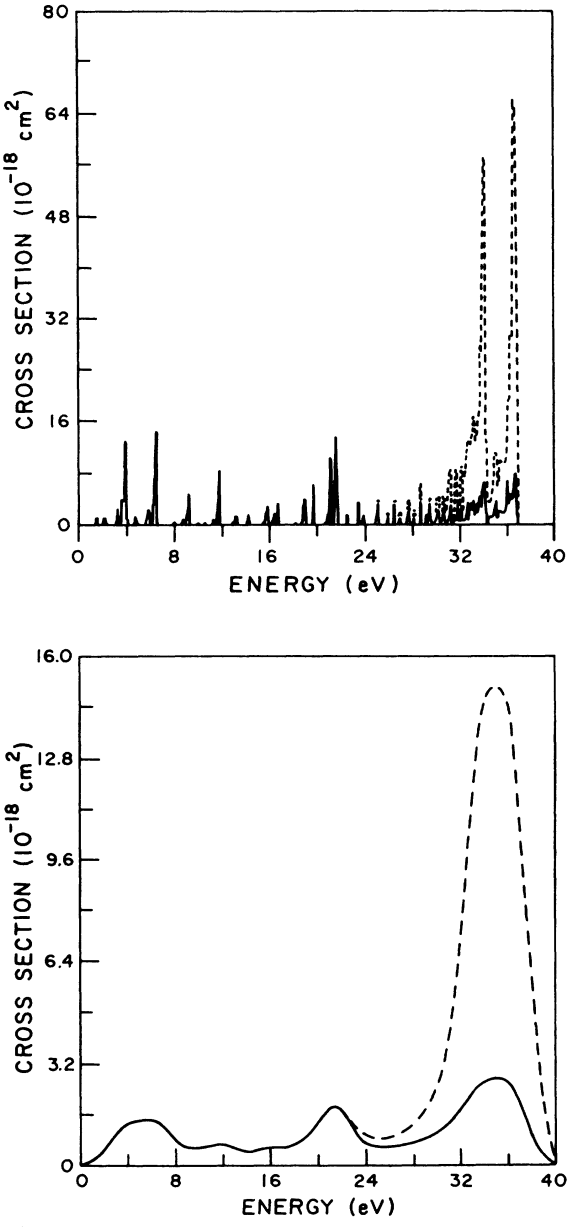

FIG. 3. $\Delta n = 0$ energy-averaged dielectronic-recombination cross section for Fe^{15+} as a function of energy. ——, cross section in the absence of a field; — — —, cross section with a field of 10 kV/cm. The upper figure shows the cross section for a bin width of 0.136 eV and the lower figure shows the cross section convoluted with a 3-eV Gaussian.

plex ($l' \geq 1$) which, as mentioned in Sec. II, was calculated including the effects of configuration interaction. These levels can all autoionize to the $3s_{1/2}$ level; in addition, levels from the $4p4d$, $4p4f$, $4d^2$, $4d4f$, and $4f^2$ configurations can also autoionize to the $3p_{1/2}$ and $3p_{3/2}$ levels, which greatly reduces the associated DR cross sections. They can radiate to the $3l''4l'$ bound levels, with $l''=l\pm1$ and to lower levels of $4l''4l'$, where $l''=l-1$ and only $4s^2$ is bound; the radiative rates for the latter transitions are quite small, and can be ignored.

The $4lnl'$ configurations with $n \geq 5$ can autoionize to the $3s_{1/2}$, $3p_{1/2}$, and $3p_{3/2}$ levels, and for $l \geq 1$ and high enough values of n, to the levels of $4l''$ with $l'' < l$. They can radiate to the bound configurations $3l''4l$, with $l''=l'\pm1$; $3l''nl'$, with $l''=l\pm1$; and to lower levels of the autoionizing configurations $4l''nl'$, with $l''=l-1$. The cross sections associated with the $4lnl'$ configuration are relatively small (at least partially due to the $4lnl' \rightarrow 3p$ autoionizing transitions) and fall off rapidly with n.

The energy-averaged cross section associated with the $\Delta n = 1$ transition as a function of electron energy is shown in the upper portion of Fig. 5. The large resonance at very low electron energy is due to the $4s4p\ ^3P_{0,1,2}$ levels and the contributions from all levels of the $4l4l'$ configurations occur between 1.6 and 80 eV. The field effects which occur only in states with high values of n are too small to be seen on the scale of this figure. Nevertheless, it is interesting to note that for the $4lnl'$ configurations, the field actually decreases the size of the cross section for many of the high-lying resonances. When the only allowed autoionizing transitions are to the initial configuration, and the autoionizing rates for the lower values of l (in the absence of a field) are larger than the radiative rates, the field will always tend to enhance the cross section by redistributing the angular momentum in such a way as to increase the effective number of recombination channels.[4] The size of the field enhancement of the cross

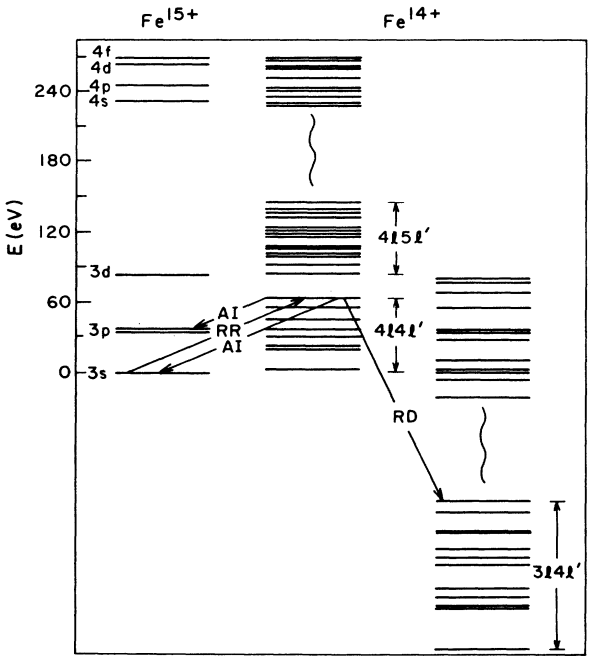

FIG. 4. Schematic energy-level diagram showing the transitions associated with $\Delta n = 1$ dielectronic recombination in Fe^{15+}. The notation is the same as that in Fig. 1.

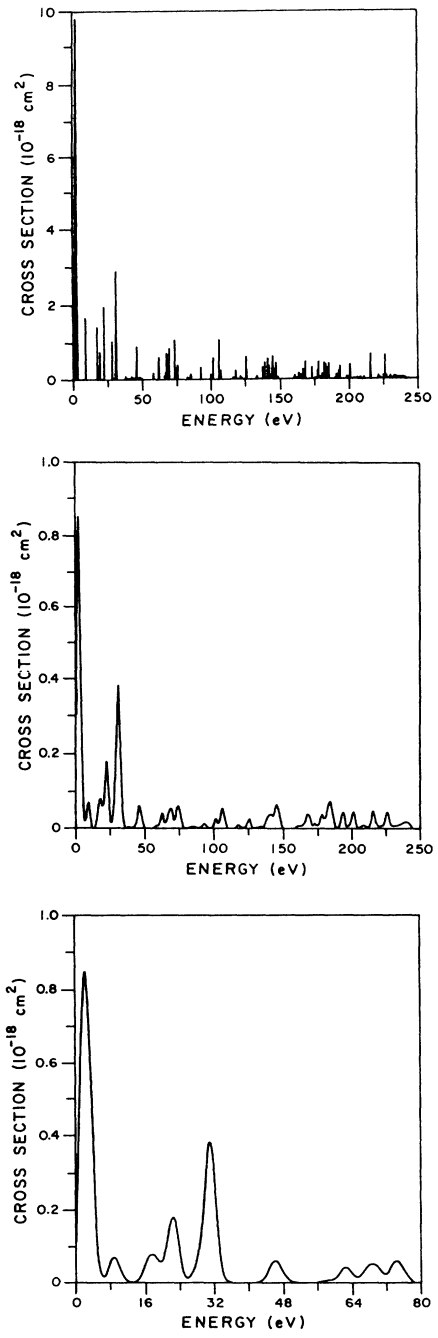

FIG. 5. $\Delta n = 1$ energy-averaged dielectronic-recombination cross section for Fe^{15+} as a function of energy. The top figure shows the cross section for a bin width of 0.136 eV and the lower two figures show the cross section convoluted with a 3-eV Gaussian. Field effects are too small to be seen on the scale of these graphs.

section will then depend only on the size of the autoionizing rates, relative to the radiative rates, after they have been modified by the field. However, when there are additional autoionizing channels possible, as there are with the $4lnl'$ configurations, the field will also redistribute the autoionizing rates to the excited configurations among the various doubly excited states; whether this will result in a decrease or increase in the cross section depends in a complicated way on the relative size of the autoionizing rates for transitions to the initial configuration versus all others.

The $\Delta n=1$ cross section convoluted with a 3-eV Gaussian is shown over the full energy range in the middle portion of Fig. 5, and also between 0 and 80 eV in the bottom portion of the figure. As can be seen, in comparison to the contributions from the $\Delta n=0$ transition, the only significant contributions occur below 40 eV. Therefore, in Fig. 6, we show the total convoluted DR cross section in this energy range, including the contributions from the $\Delta n=0$ and $\Delta n=1$ excitations. As can be seen by comparing this figure with that in the lower portion of Fig. 3, the contributions from the $\Delta n=1$ excitations are relatively small, with the only noticeable addition to the total cross section occurring at about 3 eV. Since the contributions from the $\Delta n\geq 2$ excitations, which will occur well beyond this energy range, will be even smaller than those shown in Fig. 5, this can effectively be considered the total DR cross section for this ion.

B. Dielectronic recombination in Fe^{23+}

Lithiumlike iron is the most interesting of the three ions we have considered in this paper. It exhibits field effects, although significantly smaller than those in Fe^{15+}; the spectrum of its recombination resonances is influenced much more by the spin-orbit interaction in the core electron; it has very large narrow peaks in the DR cross section at low energy; and the cross sections associated with the $\Delta n=0$ and $\Delta n=1$ excitations are completely separated in energy. A schematic energy-level diagram associated with the $\Delta n=0$ excitations is shown in Fig. 7. The $2p_{1/2}nl$ sequence for $n\geq 13$ can autoionize to the $2s_{1/2}$ level and can radiate to the bound configurations $2snl$ and $2p_{1/2}n'l'$ with $n'\leq 12$. The $2p_{3/2}nl$ sequence can autoionize to the $2s_{1/2}$ level for $n\geq 11$ and also the $2p_{1/2}$ level for $n\geq 21$, and can radiate to the bound configurations $2snl$ and $2p_{3/2}n'l'$ for $n'\leq 10$.

The energy-averaged cross sections for these two sequences as a function of n, with and without an external field, are shown in Fig. 8. Perhaps the most striking feature in this figure is the unusual shape of the field-mixed $2p_{3/2}nl$ curve. In the presence of a field, the difference in magnitude between the cross sections for the $2p_{3/2}nl$ and the $2p_{1/2}nl$ configurations is quite small at large n, while in the absence of a field, the cross section for $2p_{3/2}nl$ is about 1.8 times the cross section for $2p_{1/2}nl$. Since there are twice as many states in the $2p_{3/2}nl$ configurations, one might expect the ratio of cross sections at high n to be nearly equal to 2. The slightly lower value in the no-field case is due both to the variation of the cross sections with energy and the effect of the $2p_{3/2}nl\rightarrow 2p_{1/2}$ autoionizing channel, which appears to be small. The fact that this ratio is only about 1.1 in the presence of a field, indicates that the field modified the

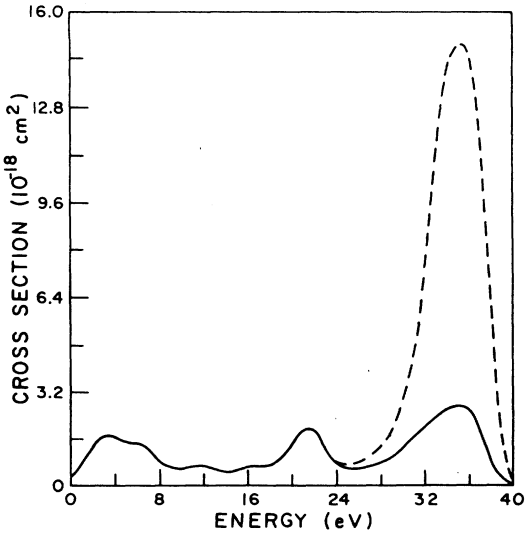

FIG. 6. Energy-averaged cross section for Fe^{15+} as a function of energy, including both $\Delta n=0$ and $\Delta n=1$ excitations, convoluted with a 3-eV Gaussian. The notation is the same as that in Fig. 3.

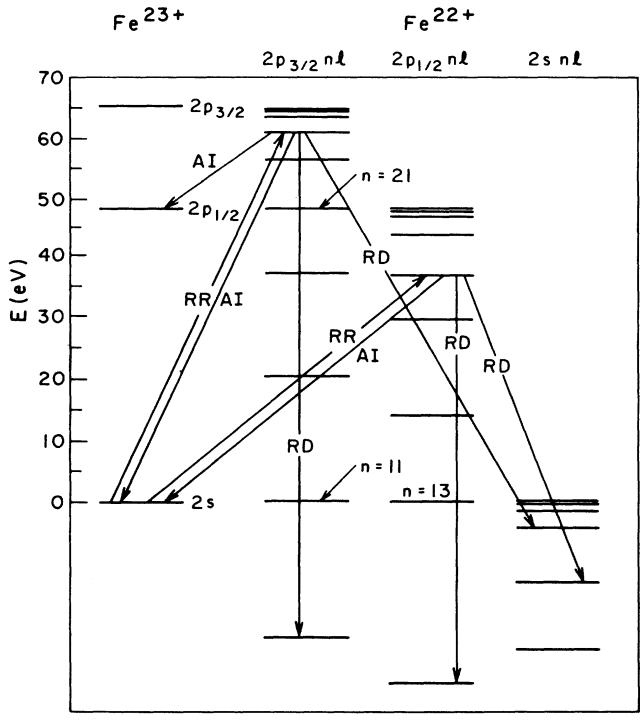

FIG. 7. Schematic energy-level diagram showing the transitions associated with $\Delta n=0$ dielectronic recombination in Fe^{23+}. The notation is the same as that shown in Fig. 1.

$2p_{3/2}nl \rightarrow 2p_{1/2}$ autoionizing rates in such a way as to have a much more pronounced effect on reducing the cross section for the $2p_{3/2}nl$ configurations. This has been verified by repeating the calculation in the field without the intercombination autoionizing transitions. In this case the ratio of these cross sections increased to a value of 1.9. Again, fields can cause some rather unusual effects when autoionizing transitions to excited configurations are energetically possible, and in this case, the influence of the field on the intercombination autoionizing transitions appears to reduce the field enhancement by about 25%.

The $\Delta n = 0$ energy-averaged cross section, in the absence of a field, as a function of electron energy is shown in the top portion of Fig. 9. As can be seen, the cross section is completely dominated by the low-lying resonances; however, it is important to note that the strength of these resonances is determined by the size of the radiative rates for type-2 transitions, involving the Rydberg electron. If only the type-1 transitions had been included in the calculation, the magnitude of the sharp peaks in the cross section near threshold would have been reduced by more than an order of magnitude. The very large peak at approximately 5 eV is due to an unresolved combination of states from the $2p_{3/2}11l$ and $2p_{1/2}13l$ configurations. The next two peaks are due to $2p_{1/2}14l$ and $2p_{3/2}12l$, respectively. With this information, it is fairly easy to follow the two sequences up the Rydberg series. The $2p_{3/2}$ series limit at 65 eV is quite apparent; however, on the scale of this graph it is impossible to distinguish the $2p_{1/2}$ limit at 48 eV.

Finally, in the bottom portion of Fig. 9, we show the energy-averaged cross sections, with and without the electric field, convoluted with a 3-eV Gaussian. It is still possible to distinguish the largest resonances at low energy, and the contributions from the high-n resonances near the two series limits are still well resolved. The field only affects the cross sections near the series limits and there the enhancement is about a factor of 2. An experiment is currently being planned on Fe^{23+}, and there is optimism that an electron distribution comparable to the one employed here may be possible.[14]

The DR cross sections associated with the $2s \rightarrow 3l$ excitations in Fe^{23+} were also calculated, and the energy-level diagram for this system is shown in Fig. 10. The $3lnl'$ configurations can autoionize to the $2s_{1/2}$, $2p_{1/2}$, and $2p_{3/2}$ levels, and for $l \geq 1$ and high enough values of n, to the levels of $3l''$ with $l'' < l$. They can radiate to the

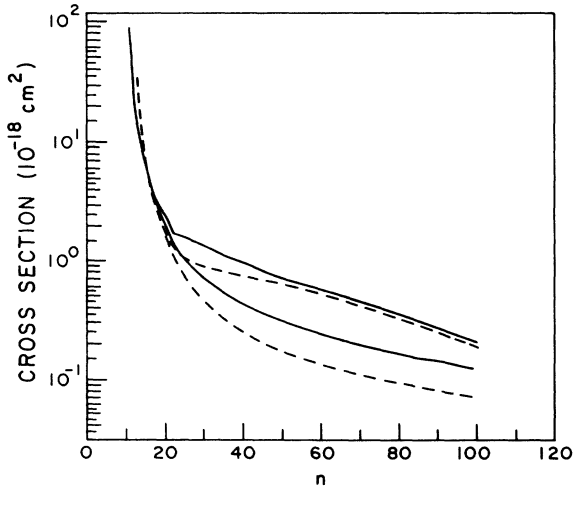

FIG. 8. $\Delta n = 0$ energy-averaged cross sections for Fe^{23+} as a function of n. ——, curve for the $2p_{3/2}nl$ configurations; — — —, curve for the $2p_{1/2}nl$ configurations. The upper two curves are for a field of 10 kV/cm while the lower two curves are for no field.

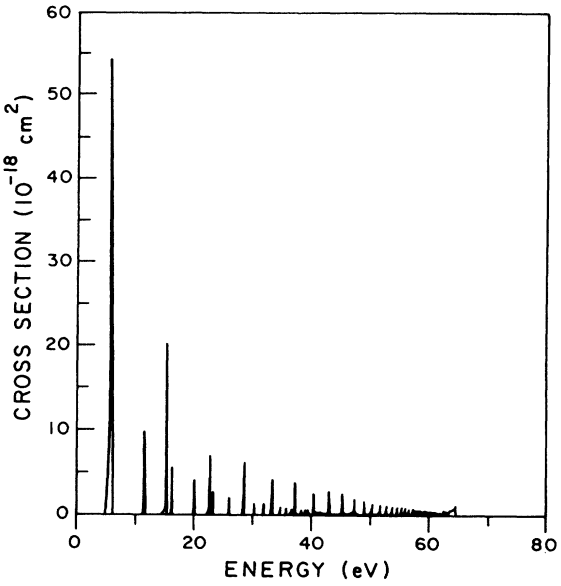

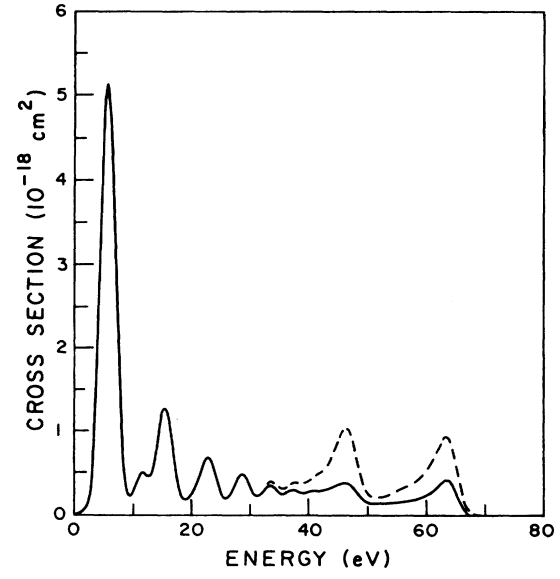

FIG. 9. $\Delta n = 0$ energy-averaged cross section for Fe^{23+} as a function of energy. The notation is the same as that for Fig. 3.

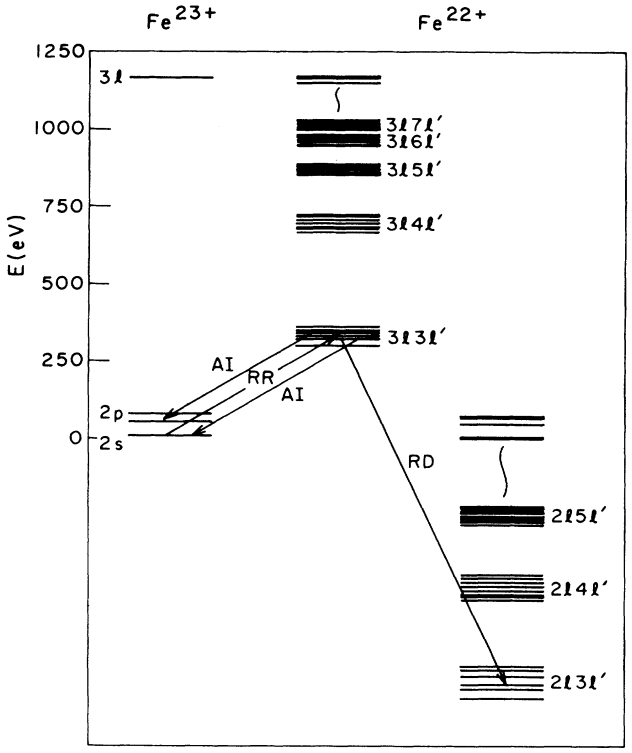

FIG. 10. Schematic energy-level diagram showing the transitions associated with $\Delta n = 1$ dielectronic recombination in Fe^{23+}. The notation is the same as that in Fig. 1.

bound configurations $2l''nl'$ with $l'' = l \pm 1$ and $2l''3l$ with $l'' = l' \pm 1$, and to lower levels of the autoionizing configurations $3l''nl'$ with $l'' = l - 1$. The energy-averaged cross section for these transitions convoluted with a 3-eV Gaussian is shown in Fig. 11. As can be seen, compared to the $\Delta n = 0$ transitions, this cross section is relatively small and may be hard to measure in any future experiments. However, it is important to keep in mind that $\Delta n \geq 1$ transitions can still make large contributions to, or even dominate, the total dielectronic-recombination-rate coefficients at temperatures of importance in laboratory and astrophysical plasmas (see, for example, Ref. 12).

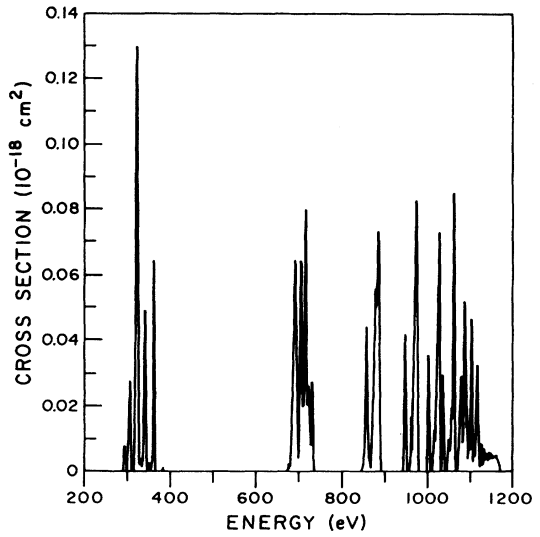

FIG. 11. $\Delta n = 1$ energy-averaged cross section in Fe^{23+} as a function of energy convoluted with a 3-eV Gaussian. The field effects are too small to be seen on the scale of this graph.

Field effects are too small to be seen on the scale of Fig. 11. Starting with the lowest energy complex of resonances associated with the $3l3l'$ configurations, it is possible to distinguish peaks due to the configurations $3lnl'$ up to $n = 11$. The sudden drop in cross section above this point is due to the fact that the strongest radiative transitions are to the $2pnl'$ configurations and these were assumed to become autoionizing for $n \geq 12$. (From our consideration of the $\Delta n = 0$ transitions, we know $2p_{3/2}nl'$ actually becomes autoionizing at $n \geq 11$, while $2p_{1/2}nl'$ becomes autoionizing for $n \geq 13$; however, DRFEUD does not take into account the energy splittings within the final configurations involved in radiative transitions, and therefore, this appears to be a reasonable compromise.)

C. Dielectronic recombination in Fe^{25+}

The last ion in our study is hydrogenlike iron. Systems which will not be influenced by external fields are of interest for future experimental investigations; since the lowest energy excitations from the ground state in Fe^{25+} involve $\Delta n = 1$ transitions, we would not expect dielectronic recombination in this ion to be affected significantly by electric fields. Predictions regarding the magnitude of this cross section are therefore important.

The schematic energy-level diagram for the $\Delta n = 1$ transitions in Fe^{25+} is shown in Fig. 12. The doubly ex-

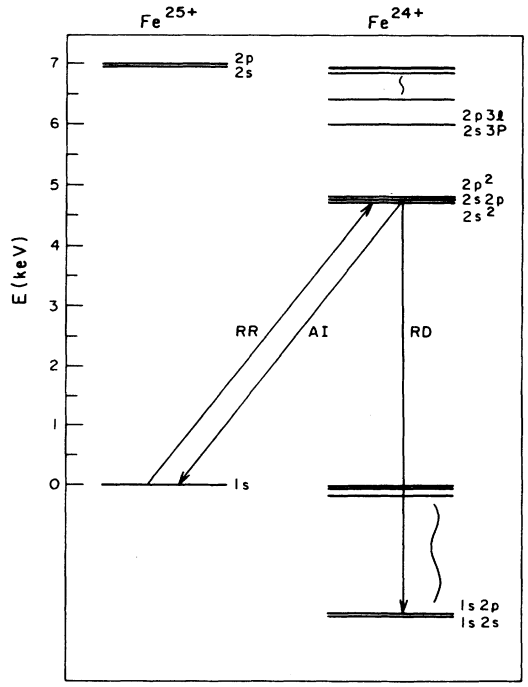

FIG. 12. Schematic energy-level diagram showing the transitions associated with $\Delta n = 1$ dielectronic recombination in Fe^{25+}. The notation is the same as in Fig. 1.

cited configurations $2lnl'$ can only autoionize back to the $1s_{1/2}$ ground state, with the exception of $2p_{3/2}nl$ which can also autoionize to both the $2s_{1/2}$ and $2p_{1/2}$ levels for $n \geq 21$. Of the $2snl$ configurations, only the $2snp$ sequence can radiate to a bound configuration, and then only to $1s2s$. The only exception to this is $2s^2$, which radiates to $1s2p$ by mixing strongly with $2p^2$. On the other hand, the $2pnl$ configurations can radiate to $1snl$, and, therefore, will dominate the cross section for higher values of n.

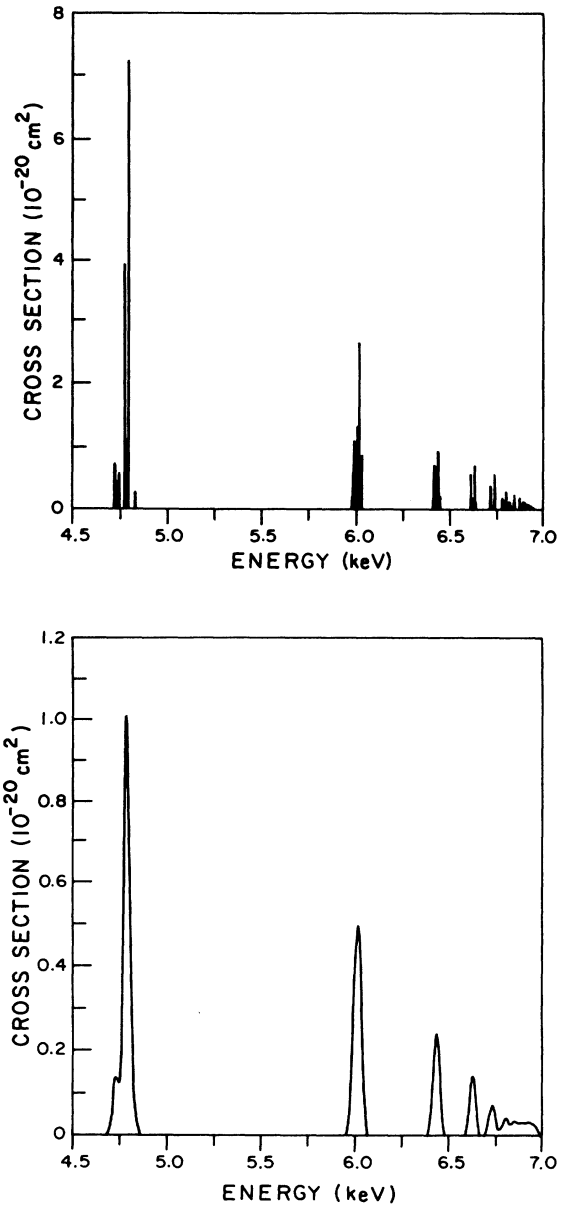

FIG. 13. $\Delta n = 1$ dielectronic-recombination cross section in Fe^{25+} as a function of energy. In the top figure the cross section has been convoluted with a 3-eV Gaussian, and in the bottom figure the cross section has been convoluted with a 30-eV Gaussian. The field effects are too small to be seen on the scale of these graphs.

The energy-averaged cross section convoluted with a 3-eV Gaussian and then a 30-eV Gaussian is shown in the top and bottom portions of Fig. 13, respectively. As we would expect, the cross section is dominated by the lowest-lying resonances, and the field effects are far too small to be seen on the scale of this graph. The resonances associated with each of the complex of configurations $2lnl'$, from $n=2$ through $n=7$, are clearly visible and easily resolved. However, it is disappointing that the size of the predicted cross section indicates that dielectronic recombination in Fe^{25+} would be very difficult to measure with any reasonable electron energy distribution.

IV. DISCUSSION AND CONCLUSIONS

We have calculated the dielectronic-recombination cross sections for Fe^{15+}, Fe^{23+}, and Fe^{25+}, in the isolated-resonance, distorted-wave approximation, including the effects of external fields. For both Fe^{23+} and Fe^{25+} the dielectronic-recombination cross sections are dominated by low-lying resonances, and even in Fe^{15+}, they are quite important; furthermore, the strength of these resonances is determined primarily by radiative transitions in which the Rydberg electron is the active electron. The field effects are only appreciable in the dielectronic-recombination transitions associated with $\Delta n = 0$ excitations, and even then they decrease rapidly with ionization stage. It appears from these calculations that, in the more highly ionized systems of interest in laboratory and astrophysical plasmas, external electric fields may have a relatively small effect on the total dielectronic-recombination rates; however, additional calculations on other species are needed to confirm this point.

As mentioned in Sec. II, we employ the isolated-resonance approximation in these calculations. In the absence of external fields, the effect of overlapping resonances on the magnitude of dielectronic-recombination cross sections, especially for high values of n, is still not fully understood; however, calculations using multichannel quantum-defect theory seem to be in general agreement with those obtained from the isolated-resonance approximation.[19,20] The effects of interference between resonances becomes more of a problem in the presence of a field, where the spacing between many of the possible interfering resonances, after Stark splitting, will be less than the resonance widths. Recently, Sakimoto[21] and independently, Harmin[22] have extended the multichannel quantum-defect theory of dielectronic recombination by Bell and Seaton[19] to include the effects of electric fields. Both employ these formulations to perform model calculations of dielectronic recombination in the presence of a field. However, at this stage, it is difficult to gauge how the field enhancement predicted from this new theory will differ from that predicted by the diagonalization technique, in conjunction with the isolated-resonance approximation, as employed here. The critical test will come when the new formalism is applied to Mg^+ where detailed experimental[1] and theoretical[8,9] results as a function of field strength already exist.

One very interesting result which comes out of

Harmin's calculation is that for n values above the Inglis-Teller limit,[23] where twice the maximum Stark shift is equal to the separation between levels with adjacent n values [$n \propto (q^3/3F)^{1/5}$, where F is the field strength in a.u.], interference effects tend to decrease the size of the field enhancement. As mentioned in Sec. II, our calculations do not include n mixing since this would make the diagonalization problem almost infinitely large. However, Harmin's calculations indicate that the combined effects of n mixing and interference between resonances with different n values will reduce the cross section. This may reduce, somewhat, the size of the field enhancement predicted here, but in no way would affect the conclusions drawn from our analysis.

One process which could have a direct effect on our results is nonresonant radiative recombination (RR). This is just the inverse of photoionization and can provide a background to the total recombination cross section near threshold. However, more importantly, interference between radiative and dielectronic recombination could at least in principle, be important. Recently it has been speculated that, since the RR cross section increases with the ionic charge, such interference could be especially important in highly ionized systems.[24,25] We have investigated this possibility by studying several transitions associated with the low-lying resonances in Fe^{15+} and Fe^{23+}.

We first consider the case of interference between RR and DR through the $2p_{3/2}11s$ states of Fe^{23+}. Here interference can occur between the dielectronic transitions

$$2skp \rightarrow 2p_{3/2}11s \rightarrow 2s\,11s + h\nu \tag{9}$$

and the radiative recombination transitions

$$2skp \rightarrow 2s\,11s + h\nu\ . \tag{10}$$

We first note that by far the strongest radiative transitions in the dielectronic process are not $2p_{3/2}11s \rightarrow 2s\,11s$, but rather $2p_{3/2}11s \rightarrow 2p_{3/2}np$, with $n \leq 10$, and RR cannot interfere with the latter transitions. Therefore, even if interference between the dielectronic and radiative transitions in (9) and (10) is important, this will have a very small effect on the cross section at this energy; nevertheless, it is interesting to determine the degree of interference. Alber *et al.*[24] have developed a unified treatment of radiative and dielectronic recombination for the special case of a single-electron continuum, and recently Jacobs *et al.*[26] have extended this theory to the case of multiple continua. The equation of Alber *et al.* in terms of the energy-averaged cross section for total recombination is given by

$$\bar{\sigma}_R = \frac{\sigma_{\rm RR}}{\Psi^2} + \frac{\bar{\sigma}_{\rm DR}}{\Psi} - \frac{\bar{\sigma}_{\rm DR}}{\Psi^3}\left[\frac{[1+(A_r/A_a)]^2 + 4(A_r/A_a)}{q^2}\right], \tag{11}$$

where $\sigma_{\rm RR}$ is the radiative-recombination cross section, $\bar{\sigma}_{\rm DR}$ is the energy-averaged dielectronic-recombination cross section, $\Psi = 1 + (A_r/q^2 A_a)$, and q is the Fano q parameter[27] The third term in this equation is due to the interference between the amplitudes for RR and DR. Obviously in the limit of large q, Eq. (11) reduces to $\bar{\sigma}_R = \sigma_{\rm RR} + \bar{\sigma}_{\rm DR}$.

We have calculated the values of q^2 for the $J=2 \rightarrow J=1$, $J=1 \rightarrow J=1$, and $J=1 \rightarrow J=0$ transitions associated with (9) and (10) above, and they vary from 1.2×10^3 to 1.3×10^4. Thus it is clear that the interference between RR and DR is completely negligible here.

Even though the individual values of $\sigma_{\rm RR}$ are a factor of 100 smaller than the individual values of $\bar{\sigma}_{\rm DR}$, this does not imply that the total RR cross section is negligible at this energy. It is determined by summing the individual values of $\sigma_{\rm RR}$ from all continuum states of $2sk_\varepsilon l_\varepsilon$ to all final states of the configurations $2snl$. This total can be estimated from a semiclassical hydrogenic formula due to Kramers[28] (see, for example, Ref. 16):

$$\sigma_{\rm RR} = \frac{32\pi\alpha^3 Q^4/n^3}{3\sqrt{3}k_\varepsilon^2(k_\varepsilon^2 + Q^2/n^2)}\ , \tag{12}$$

where α is the fine-structure constant, Q is the charge of the initial N-electron ion, and the cross section is in atomic units. This equation appears to give values for total radiative-recombination cross sections within 10% of those obtained from a more elaborate hydrogenic formula,[29] and results for Fe^{23+} are shown in Table I. The cross section is quite large at very low energies, and for an energy near the first large resonance at 5.0 eV, it adds about 1.0×10^{-18} cm^2 to the cross section; however, in the regions of the $2p_{1/2}$ and $2p_{3/2}$ series limits the additional contribution is less than 10%.

TABLE I. Radiative-recombination cross sections $\sigma_{\rm RR}$ for Fe^{15+} and Fe^{23+} estimated from the approximate hydrogenic formula Eq. (12).

Electron energy eV	Fe^{15+} $\sigma_{\rm RR}$ (10^{-18} cm^2)	Fe^{23+} $\sigma_{\rm RR}$ (10^{-18} cm^2)
0.50	4.134	11.909
1.00	1.911	5.692
1.50	1.204	3.665
2.00	0.864	2.672
2.50	0.666	2.086
3.00	0.537	1.702
3.50	0.448	1.431
4.00	0.382	1.231
4.50	0.332	1.077
5.00	0.292	0.956
6.00	0.234	0.776
7.00	0.194	0.650
8.00	0.165	0.557
9.00	0.142	0.486
10.00	0.125	0.430
15.00	0.075	0.268
20.00	0.052	0.190
25.00	0.039	0.146
30.00	0.030	0.117
35.00	0.025	0.097
40.00	0.021	0.082
45.00	0.017	0.071
50.00	0.015	0.063
55.00	0.013	0.057
60.00	0.012	0.050
65.00	0.011	0.045

For Fe^{15+} we considered interference of RR with the lowest energy resonance due to the $4s4p\ ^3P_{0,1,3}$ levels. Here interference is possible between the dielectronic transitions

$$3skp\ ^3P \rightarrow 4s4p\ ^3P \rightarrow 3s4s\ ^3S + h\nu \quad (13)$$

and the radiative-recombination transitions

$$3skp\ ^3P \rightarrow 3s4s\ ^3S + h\nu\ . \quad (14)$$

The rates associated with the radiative transitions $4s4p\ ^3P \rightarrow 3s4s\ ^3S$ are about 30% of the total rate from $4s4p\ ^3P$ levels, so if interference were important it would affect the size of this resonance. However, the values of q^2 are again quite large, varying from 1.6×10^3 to 5.2×10^3, and the interference is negligibly small. The RR cross sections for this ion estimated from Eq. (12) are also given in Table I. In the region of the lowest energy resonances, this process would add another 30% to the cross section, while at the high-energy peak, it would add less than 1%.

Thus we see that, for both of these ions, RR will contribute to the total recombination cross section close to threshold, and this may be detectable in future experiments. However, interference between RR and DR is completely negligible, and, therefore, we would expect that the size of the low-lying dielectronic-recombination resonances are predicted with reasonably good accuracy by these calculations. In Fe^{25+}, both radiative recombination and interference between RR and DR will be completely negligible in the relatively high-energy range where DR begins.

ACKNOWLEDGMENTS

We wish to thank R. D. Cowan for making his atomic structure programs available to us. In addition, we would like to thank J. Cooper for discussions regarding interference effects in recombination, and A. Müller, S. Datz, and P. F. Dittner for discussions regarding possible future DR experiments. The first author would like to thank the Joint Institute for Laboratory Astrophysics for their hospitality and financial support through the JILA Visiting Fellows Program. This work was partially supported by the Office of Fusion Energy, U. S. Department of Energy, under Contract No. DE-AC05-84OR21400 with Martin Marietta Energy Systems, Inc. and Contract No. DE-FG05-86ER53217 with Auburn University.

*Permanent address: Department of Physics, Rollins College, Winter Park, Florida 32789.

[1]A. Müller, D. S. Belić, B. D. DePaola, N. Djuric, G. H. Dunn, D. W. Mueller, and C. Timmer, Phys. Rev. Lett. **56**, 127 (1986).

[2]V. L. Jacobs, J. Davis, and P. C. Kepple, Phys. Rev. Lett. **37**, 1390 (1976).

[3]K. LaGattuta and Y. Hahn, Phys. Rev. Lett. **51**, 558 (1983).

[4]D. C. Griffin, M. S. Pindzola, and C. Bottcher, Oak Ridge National Laboratory Report No. ORNL/TM-9478, 1985 (unpublished).

[5]D. C. Griffin, M. S. Pindzola, and C. Bottcher, *Atomic Excitations and Recombination in External Fields,* edited by M. H. Nayfeh and C. W. Clark (Harwood Academic, New York, 1985).

[6]K. J. LaGattuta, J. Phys. B **18**, L467 (1985).

[7]D. C. Griffin, M. S. Pindzola, and C. Bottcher, Phys. Rev. A **33**, 3124 (1986).

[8]C. Bottcher, D. C. Griffin, and M. S. Pindzola, Phys. Rev. A **34**, 860 (1986).

[9]K. LaGattuta, I. Nasser, and Y. Hahn, Phys. Rev. A **33**, 2782 (1986).

[10]K. J. LaGattuta and Y. Hahn, Phys. Rev. A **30**, 316 (1984).

[11]D. J. McLaughlin and Yukap Hahn, Phys. Rev. A **29**, 712 (1984).

[12]L. J. Roszman, Phys. Rev. A **35**, 2122 (1987).

[13]J. DuBau, A. H. Gabriel, M. Loulergue, L. Steenman-Clark, and S. Volonté, Mon. Not. R. Astron. Soc. **195**, 705 (1981).

[14]A. Müller (private communication).

[15]S. Datz and P. F. Dittner (private communication).

[16]R. D. Cowan, *The Theory of Atomic Structure and Spectra* (University of California, Berkeley, 1981).

[17]D. C. Griffin, M. S. Pindzola, and C. Bottcher, Phys. Rev. A **31**, 568 (1985).

[18]R. J. Damburg and V. V. Kolosov, J. Phys. B **12**, 2637 (1979).

[19]R. H. Bell and M. J. Seaton, J. Phys. B **18**, 1589 (1985).

[20]A. K. Pradhan, Phys. Rev. A **30**, 2141 (1984).

[21]K. Sakimoto, J. Phys. B **19**, 3011 (1986), and private communication.

[22]D. A. Harmin, Phys. Rev. Lett. **57**, 1570 (1986).

[23]D. R. Inglis and E. Teller, Astrophys. J. **90**, 439 (1939).

[24]G. Alber, J. Cooper, and A. R. P. Rau, Phys. Rev. A **30**, 2845 (1984).

[25]A. R. P. Rau, *Atomic Excitation and Recombination in External Fields,* edited by M. H. Nayfeh and C. W. Clark (Harwood Academic, New York, 1985).

[26]V. L. Jacobs, J. Cooper, and S. L. Haan (private communication).

[27]U. Fano, Phys. Rev. **124**, 1866 (1961).

[28]H. A. Kramers, Philos. Mag. **46**, 836 (1923).

[29]H. S. W. Massey, *Electronic and Ionic Impact Phenomena,* 2nd ed. (Oxford University Press, London, 1969), Vol. II.